

Examination of level density prescriptions in the interpretation of high energy γ -ray spectra

Srijit Bhattacharya,¹ Deepak Pandit,² Balaram Dey,² Debasish Mondal,²
S. Mukhopadhyay,² Surajit Pal,² A. De,³ and S. R. Banerjee^{2,*}

¹*Department of Physics, Barasat Govt. College, Barasat, N 24 Pgs, Kolkata-700124, India*

²*Variable Energy Cyclotron Centre, 1/AF, Bidhannagar, Kolkata-700064, India*

³*Department of Physics, Raniganj Girls' College, Raniganj-713358, India*

(Dated: November 6, 2014)

High energy γ -ray spectra measured by our group involving the compound nuclei (CN) ^{63}Cu at excitation energy (E^*) ~ 36 MeV with average angular momentum (J) = 12 - 17 \hbar , ^{97}Tc at $E^* \sim 29$ - 50 MeV with J = 12 - 14 \hbar , ^{113}Sb at $E^* = 109$ MeV and 121 MeV with $J = 49$ - 59 \hbar and ^{201}Tl at $E^* = 39.5, 47.5$ MeV with $J = 18$ - 24 \hbar have been analyzed utilizing the level density prescriptions of (i) Ignatyuk, Smirenkin and Tishin (IST), (ii) Budtz-Jorgensen and Knitter (BJK), and (iii) Kataria, Ramamurthy and Kapoor (KRK). These three prescriptions have been tested for correct statistical model description of high energy γ -rays in the light of extracting the giant dipole resonance (GDR) parameters at low excitation energy and spin where shell effects might play an important role as well as at high excitation energy where shell effects have melted. Interestingly, only the IST level density prescription could explain the high energy γ -ray spectra with reasonable GDR parameters for all the four nuclei.

I. INTRODUCTION

One of the most exciting topics in contemporary nuclear physics is the study of nuclear structure under extreme conditions of nuclear temperature (T) and angular momentum (J). The giant dipole resonance (GDR), an archetypical example of collective vibrational mode built on excited nuclear states, provides us the insight of exotic nuclear shapes and structure [1–3]. Ardent experimental and theoretical interests [4–22] can be seen over the years in studying the properties of the GDR built on excited states in nuclei as this collective mode is strongly coupled to nuclear damping and shape degrees of freedom. The strength (S_{GDR}), centroid energy (E_{GDR}) and width (Γ_{GDR}) are the parameters that describe a GDR strength function. The knowledge in E_{GDR} provides better understanding of the symmetry energy of nuclear matter while the systematic study of Γ_{GDR} with T sheds light on the characteristics of damping prevailing within the nuclear matter as well as the evolution of deformations embodied within it [23].

Measurement of high energy γ -rays ($E_\gamma = 8$ - 20 MeV) from the decay of hot compound nucleus (CN) is one of the most important probes for studying the GDR in excited nuclei. To understand the properties of the GDR parameters in excited nuclei, the characterization of the measured high energy γ -rays and its comparison with the predictions of theoretical statistical model related to CN decay are absolutely necessary. However, the acceptability of any statistical model prediction depends on its essential ingredient, the nuclear level density, which is also the central source of uncertainty in analyzing nuclear re-

actions and in reliable extraction of the GDR quantities i.e S_{GDR} , E_{GDR} and Γ_{GDR} .

It is an important fact that the level density of excited nuclei is strongly influenced by the nuclear shell structure that melts down with the increase in excitation energy (E^*) of the nucleus. Although for high spin and high E^* the shell structure might not be melted near the yrast line. The reliable extraction of the GDR Lorentzian not only depends on the statistical model predictions for the region $E_\gamma = 8$ -20 MeV of the high energy γ -ray spectrum but also on the statistical part ($E_\gamma \leq 8$ MeV) of the spectrum. The statistical part is highly sensitive to the level density of the decaying nuclei, especially in the later part of the decay chain where shell effect is extremely important. Angular momentum (J) as well as the evolution of nuclear deformation in the CN decay chain also play leading roles in the modification of nuclear level density. Therefore, the statistical model must include a proper level density formalism as input, which can take care of all these facts.

The basic nuclear level density formula, derived from the backshifted Fermi gas model and based on the pioneering work of Bethe [24], is given by

$$\rho(E^*, J) = \frac{2J+1}{12I^{3/2}} \sqrt{a} \frac{\exp(2\sqrt{aU})}{U^2} \quad (1)$$

where $U = E^* - \Delta - J(J+1)\hbar^2/2I$ is the available thermal energy. The effective moment of inertia of the compound nucleus is taken as $I = I_0(1 + \delta_1 J^2 + \delta_2 J^4)$, where I_0 is the spherical rigid body moment of inertia while δ_1 and δ_2 are the deformability coefficients. The excitation energy is back-shifted by the pairing energy $\Delta = 12/\sqrt{A}$, A being the mass number of the nucleus. a is the level density parameter and is taken as an adjustable free parameter.

In the Fermi gas model the level density depends on the level density parameter a which, in turn, is related to

*e-mail:srb@vecc.gov.in

the finite size effect of the nuclear matter, the effective mass of the nucleon and the number of single particle levels near the Fermi surface. All of these depend on nuclear deformation, shell structure of the nucleus and also how the shell structure gradually melts with the increase in E^* of the nucleus. Pühlhofer's [25] statistical model code CASCADE includes formulation of level density parameter a as per Dilg [26] for $E^* < 10$ MeV. For $E^* > 20$ MeV, $a = A/k$ was used, based on the liquid drop model, where k is user dependent free inverse level density parameter and A is the nuclear mass. For E^* ranging from 10 - 20 MeV, linear interpolation of a and Δ is done in midway between the parametrization of Dilg and that of the liquid drop model. But the non-inclusion of the proper treatment of the shell corrections and its washing out at higher excitation energies along with the effect of nuclear deformation induces large uncertainty [5] in explaining the high energy γ -ray spectra when Dilg formulation is used.

An ideal level density prescription should describe level density correctly starting from lower to higher E^* at different J values. It should also incorporate shell effects at lower E^* smoothly connecting to the liquid drop behavior of the nucleus at higher E^* and it must describe the high energy γ -ray spectra faithfully. The existing level density formulation by Ignatyuk, Smerekin and Tishin (IST) [27] is quite popular as it can predict high energy γ -rays at different excitations. Besides IST, a few other modified theoretical as well as empirical level density prescriptions also exist in the literature. Two such level density prescriptions are of Kataria, Ramamurthy and Kapoor (KRK) [28] and Budtz-Jorgensen and Knitter (BJK) [29]. Dioszegi et al [30] have shown a comparative study between Dilg, IST and BJK level density formalisms for $A = 110 - 130$ over the excitation energy range 58 - 62 MeV ($T = 1.98 - 2.23$ MeV) and angular momentum 16.9-20.9 \hbar by matching experimental high energy γ -ray spectra with CASCADE predictions. They pointed towards the superiority of IST level density over the others (Dilg and BJK) in the said E^* region and also could not find any change of the GDR parameters even after including different level density prescriptions within the statistical model. However, they did not test the IST level density prescription at lower temperatures where the shell structure is important. Moreover, the other two prescriptions (KRK and BJK) have never been used in describing the high energy γ -ray spectra for different nuclei at different excitation energies.

In this work, the KRK, BJK and IST level density formalisms are rigorously tested at lower excitation energy ranges $E^* \sim 29 - 50$ MeV and lower spin (12 - 17 \hbar) for the CN ^{97}Tc and ^{63}Cu as well as at higher excitation energy $E^* \sim 109 - 121$ MeV and higher spin (49 - 59 \hbar) for ^{113}Sb . In addition, the applicability of IST and KRK level density prescriptions are also investigated on the high energy γ -ray spectra of ^{201}Tl , in which the ground state shell correction energy is larger than ^{63}Cu , ^{97}Tc and ^{113}Sb . Here, the advantage of populating these non-

fissioning nuclei having ground state spherical is that the user-dependent free parameters in CASCADE decrease considerably and a one-component GDR strength function can be extracted reliably. As a result, it becomes much easier to test the CASCADE predictions giving full emphasis only on the level density input. Moreover, we chose KRK level density rather than Dilg et al, as the former incorporates the shell structure of nuclei at lower E^* and also its extrapolation to higher energies.

II. EXPERIMENTAL DETAILS

Very recently, a large amount of experimental data [12, 15, 17, 19] on high energy γ -ray ($E_\gamma = 4 - 32$ MeV) measurements have been reported in different nuclei and in varying excitation energies as well as angular momenta for studying the properties of the GDR modes in nuclei. Using the alpha beam from the K-130 cyclotron at the Variable Energy Cyclotron Centre, Kolkata, a self supporting 1 mg/cm² thick ^{93}Nb target was bombarded at the projectile energies of 28, 35, 42 and 50 MeV populating the compound nucleus ^{97}Tc at the excitation energies of 29.3, 36, 43 and 50.4 MeV, respectively [19]. The compound nuclei were populated in the angular momentum window 12 - 21 \hbar . The high energy γ -spectra were measured by means of a part (49 detectors in the form 7×7 matrix) of the LAMBDA array [31]. The array was placed at a distance of 50 cm from the target and at an angle of 90⁰ with the beam axis. The angular momentum populated by the compound nucleus was measured with a 50-element low energy γ -multiplicity detector array [32]. To measure the inverse level density parameter (k) at different energies, the evaporated neutron energy spectra were extracted by converting the time of flight data of BC501A liquid scintillators [33]. In other nuclear reactions $^4\text{He} + ^{59}\text{Co}$, $^{20}\text{Ne} + ^{93}\text{Nb}$, and $^4\text{He} + ^{197}\text{Au}$, the compound nuclei ^{63}Cu , ^{113}Sb and ^{201}Tl were populated for the beam energies of $E_{lab} = 35$ MeV, 145 and 160 MeV, 42 and 50 MeV, respectively. The details of the experiments are explained elsewhere [12, 17].

III. ADOPTED LEVEL DENSITIES

The experimental spectra of high energy γ -rays coming from the decay of the compound nuclei (^{63}Cu , ^{97}Tc , ^{113}Sb and ^{201}Tl) were fitted with the CASCADE predictions, using different level density prescriptions, folded with the detector response along with an exponential bremsstrahlung component given by $\exp(-E_\gamma/E_0)$ (E_0 is the slope parameter). The bremsstrahlung slope parameter E_0 was obtained from the systematics $E_0 = 1.1[(E_{lab} - V_c)/A_p]^{0.72}$ where E_{lab} , V_c and A_p represent the beam energy, Coulomb barrier and projectile mass, respectively [34]. Corresponding experimental angular momentum distribution, E_{GDR} , S_{GDR} and Γ_{GDR} were taken as CASCADE inputs. The GDR parameters were

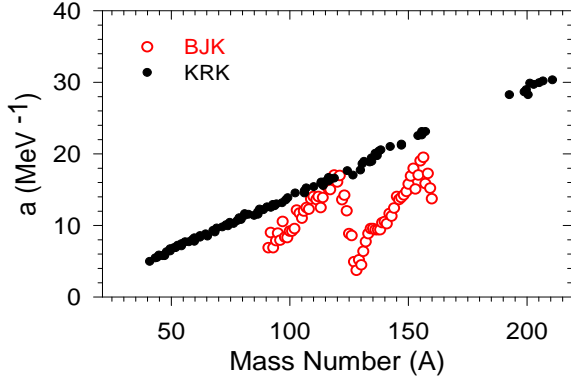


FIG. 1: (Color online) The mass dependent level density parameters calculated by Kataria (i.e, KRK) for spherical nuclei (the filled circles). The red edged open circles are the level density parameters compiled by BJK from the experimental data on spontaneous fission of ^{252}Cf .

extracted by the χ^2 best fit CASCADE predictions (in between $E_\gamma = 10\text{--}20$ MeV). For all the models, at a common beam energy, the bremsstrahlung slope parameter E_0 was kept fixed as per systematics and only the GDR strengths, widths and centroid energies were varied.

A. KRK level density prescription

The semi-empirical model proposed by KRK [28] on nuclear level density is important for statistical model of nuclear decay as it incorporates the shell effects and their E^* dependence. The excitation energy and spin dependent level density $\rho(E^*, J)$, related with state density $W(E^*)$, adopted in this model is given by:

$$\rho(E^*, J) = \frac{(2J+1)W(E^*)}{2\sqrt{(2\pi)}\sigma^3(E^*)} \exp\left(\frac{-J(J+1)}{2\sigma^2(E^*)}\right) \quad (2)$$

$$W(E^*) = C \exp S(E^*) \quad (3)$$

where σ is the spin cut-off parameter that depends on the effective moment of inertia of the nucleus. The state density $W(E^*)$ is related with entropy S , a function of excitation energy. E^* and the temperature T of the excited nucleus are interconnected by the level density parameter a . Unlike other level density formalisms, KRK propose the level density parameter as shell-independent similar to that of a nucleus under the liquid drop model. Here, the shell structure influences the level density with a ground state shell correction energy term added in the total nuclear E^* .

In KRK model, the analytical expressions of entropy and excitation energy can be achieved after detailed calculation as,

$$S = \frac{1}{3}\pi^2 g_0 T + \frac{A_1}{T} \frac{\pi^2 \omega^2 T^2 \cosh(\pi \omega T)}{\sinh^2(\pi \omega T)} - \frac{\pi \omega T}{\sinh \pi \omega T} \quad (4)$$

$$E^* = \frac{1}{6}\pi^2 g_0 T^2 + A_1 \left(\frac{\pi^2 \omega^2 T^2 \cosh(\pi \omega T)}{\sinh^2(\pi \omega T)} \right) \quad (5)$$

where A_1 , the ground state shell correction energy, depends on the fundamental frequency of oscillation of the fluctuating part in level density (ω). At large temperature limit, one gets $S = \pi^2 g_0 T/3$ and $E^* = -A_1 + \pi^2 g_0 T^2/6$, where g_0 is the density of single particle states proportional to the level density parameter a . These equations may be used as the framework to calculate the level density parameter as a function of E^* with known values of ground state shell correction energies. The constants α , β and ω_0 can be estimated by comparing the theoretical nuclear level spacing with the experimental level spacing obtained from the neutron resonance data at $E^* \sim 10$ MeV. These constants are related to the level density parameter and the frequency of shell oscillation (ω) by $a = \alpha A(1 - \beta A^{-1/3} B_s)$ and $\omega = \omega_0 A^{-1/3}$, where B_s is the surface area relative to that of a sphere of same volume. The reported best fit values were [28], $\alpha = 0.18 \text{ MeV}^{-1}$, $\beta = 1.0$ and $\omega_0 = 0.185 \text{ MeV}^{-1}$.

KRK found that the level density calculated with this model successfully agrees with the experimental data up to the excitation energy around 25 MeV for the nuclei ^{56}Fe and ^{55}Mn [35]. The mass dependent level density parameters calculated by KRK for spherical nuclei are shown in Fig 1. Unfortunately, the KRK model has not been used in the past for the extraction of GDR parameters.

B. BJK level density prescription

The second of the three nuclear level density prescriptions used in this work is that of BJK. The experimentally measured and compiled values of mass dependent level density parameters by BJK [29] for the nuclei ranging from $90 \leq A \leq 165$ are shown in Fig. 1 by red edged open circles. These level density parameters were extracted from neutron evaporation measurements in spontaneous fission of ^{252}Cf .

C. IST level density prescription

The model proposed by IST [27] involves improved E^* -dependent level density parameter a . In this model the level density parameter is given by,

$$a(U) = \tilde{a}(1 + \frac{\delta W}{U}(1 - \exp(-\gamma U))) \quad (6)$$

This parametrization incorporates the effect of nuclear shell structure at lower excitation energy and extrapolates to the smooth liquid drop behavior at higher excitation energy where the shell effect is expected to be melted. δW is the shell correction factor which is the difference between the experimental and the liquid drop masses. γ^{-1} is the rate at which shell effects melt as

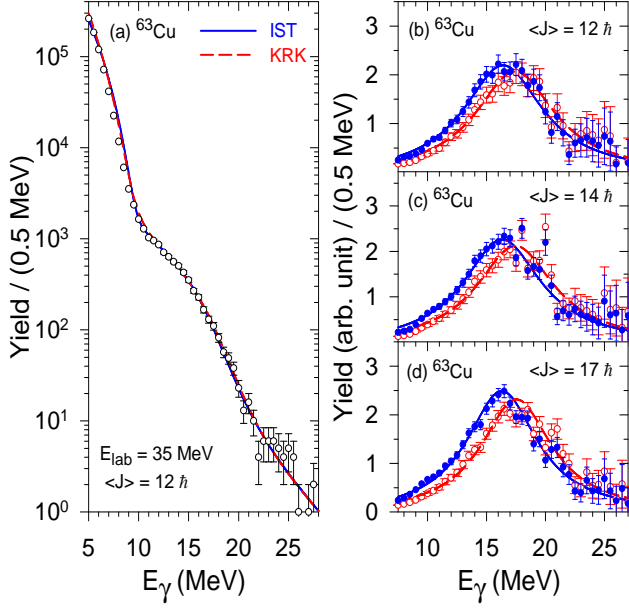


FIG. 2: (Color online) Panel (a): The experimental high energy γ -ray spectra (open circles with error bars) for the reaction $^4\text{He}+^{59}\text{Co}$ at projectile energy 35 MeV along with the CASCADE predictions utilizing KRK (red dashed line) and IST (blue continuous line) level density formalisms. Panels (b) to (d): The corresponding experimental linearized divided plots at different angular momenta IST (filled circles with blue continuous line) and KRK (open circles with red dashed line) level density prescriptions.

E^* increases and it is generally taken as 18.5 MeV. \tilde{a} is asymptotic Fermi gas level density parameter and is taken as a user dependent free parameter. In partial modification of this formula, Reisdorf [36] showed that asymptotic level density parameter depends on the mass of the compound nucleus as well as the nuclear deformation, given by:

$$\tilde{a} = 0.04543r_0^3 + 0.1355r_0^2A^{-1/3}B_s + 0.1426r_0A^{-2/3}B_k \quad (7)$$

where, B_s and B_k are the nuclear surface and curvature terms, respectively, and taken as 1 for spherical nuclei. r_0 , the nuclear radius parameter, is taken as 1.15 fm.

IV. RESULTS AND DISCUSSION

In view of the available high energy γ -ray spectra measured by our group for the compound nuclei ^{63}Cu , ^{97}Tc , ^{113}Sb and ^{201}Tl over a wide range of excitation energies 29.3 - 109 MeV and angular momenta 12-59 \hbar , we attempt here to assess the applicability of the three level density prescriptions. ^{63}Cu , ^{97}Tc and ^{113}Sb , all of them have lower ground state shell correction energies (1.86 MeV, 1.26 MeV and 1.54 MeV, respectively). On the other hand, ^{201}Tl has higher ground state shell correction energy of -8.27 MeV. While all the other three nuclei

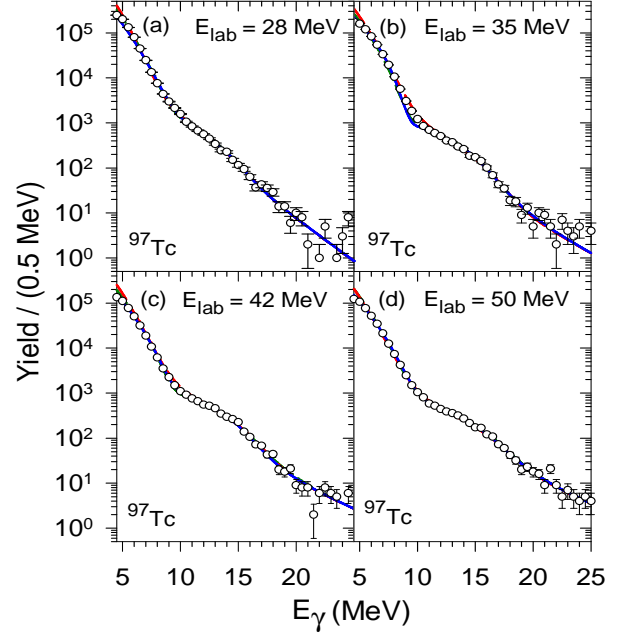


FIG. 3: (Color online) Panels (a) to (d): The experimental high energy γ -ray spectra (open circles with error bars) for the reaction $^4\text{He}+^{93}\text{Nb}$ at projectile energies 28, 35, 42 and 50 MeV along with CASCADE predictions utilizing KRK (red dashed line), BJK (green dotted-dashed line) and IST (blue continuous line) level density formalisms.

were populated at lower E^* and J , ^{113}Sb was populated at higher E^* and J values.

A. ^{63}Cu

The experimental high energy γ -ray spectrum for the compound nucleus ^{63}Cu at projectile energy 35 MeV ($E^*=36$ MeV) and CN average angular momentum $J=12$ \hbar is shown in panel (a) of Fig. 2 by open circles. The CASCADE predictions utilizing IST (blue continuous line) and KRK (red dashed line) level density prescriptions are also included in the same figure. It is highly interesting to note that both the IST and KRK level density formalisms included CASCADE represent the high-energy γ -ray spectra equally well. However, the extracted GDR centroid energies are very different. The discrepancy is evident in the linearized GDR plots shown in Fig.2b-d for $J=12, 14$ and 17 \hbar using the quantity $F(E_\gamma)Y^{\text{exp}}(E_\gamma)/Y^{\text{cal}}(E_\gamma)$, where, $Y^{\text{exp}}(E_\gamma)$ and $Y^{\text{cal}}(E_\gamma)$ are the experimental and the best fit CASCADE spectra, corresponding to a single Lorentzian function $F(E_\gamma)$. The GDR centroid energy extracted at different J using KRK prescription comes out to be 17.9 MeV. This value is slightly larger than the existing systematics of GDR built on excited state: $E_{\text{GDR}} = 18 A^{-1/3} + 25 A^{-1/6}$ [1] which predicts 17.0 MeV. On the contrary, the IST level density included CAS-

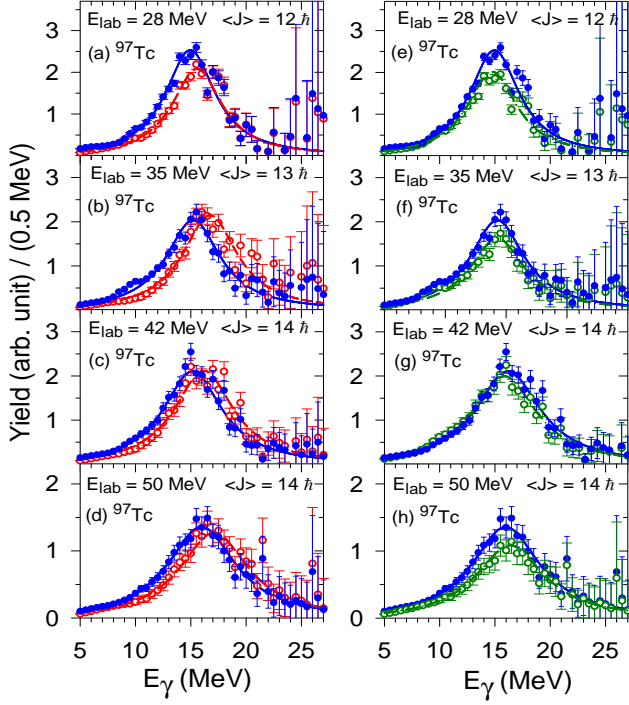


FIG. 4: (Color online) Panels (a) to (d): The experimental linearized plots for the reaction $^4\text{He} + ^{93}\text{Nb}$ at projectile energies 28, 35, 42 and 50 MeV along with CASCADE predictions utilizing KRK (open circles with red dashed line) and IST (filled circles blue continuous line) level density formalisms. Panels (e) to (h): Same as above but utilizing BJK (open circles with green dotted-dashed line) and IST (filled circles with blue continuous line) level density formalisms.

CASCADE successfully predicts the high energy γ -ray spectra for ^{63}Cu with E_{GDR} coming out between 16.7 to 16.9 MeV, much closer to the systematics. Unfortunately, it was not possible to test BJK level density for the nucleus ^{63}Cu as lower mass $A = 63$ does not fall under the mass distribution of ^{252}Cf fission fragment.

B. ^{97}Tc

The experimental high energy γ -ray spectra for ^{97}Tc at projectile energies of 28, 35, 42 and 50 MeV corresponding to $E^* = 29.3, 36.0, 43.0$ and 50.4 MeV are shown in the panels a-d of Fig. 3 along with CASCADE predictions utilizing KRK (red dashed lines), BJK (green dotted-dashed line) and IST (blue continuous line) level density prescriptions. For better understanding of the GDR strength function, the corresponding linearized divided plots have also been shown in Fig. 4. The comparison between IST and KRK prescriptions is demonstrated in the panels (a)-(d) of the figure, while similar comparison between IST and BJK prescriptions is shown in the panels (e)-(h) of the same figure. The corresponding CN average J -values are also quoted in all the figures.

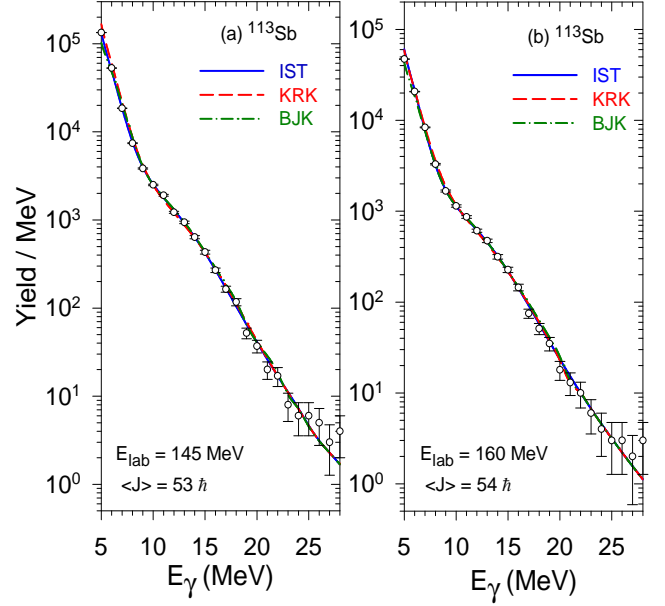


FIG. 5: (Color online) (a) The experimental high energy γ -ray spectrum (open circles with error bars) for the reaction $^{20}\text{Ne} + ^{93}\text{Nb}$ at projectile energy 145 MeV along with CASCADE predictions exploiting KRK (red dashed line), BJK (green dotted-dashed line) and IST (blue continuous line) level density formalisms. (b) Same as (a) but for the reaction at projectile energy 160 MeV.

Here the linearized GDR Lorentzians once again corroborate the similar trend observed in ^{63}Cu . The KRK prescription explains the GDR line shape well but with higher values of E_{GDR} . The extracted best fit E_{GDR} is found to be lying between 17.0-17.5 MeV, much higher than the value of 15.6 MeV as per the existing systematics, except for $E_{\text{lab}} = 28$ MeV in which the best fit value comes out to be 15.8 MeV closer to the systematics. It is worthwhile to mention that not only the CN ^{97}Tc is populated in lower excitation energy ranges but also the compound nuclear angular momentum lies in lower side between 12 to 14 \hbar .

The statistical model code CASCADE using BJK prescription can predict high energy γ -ray spectra reasonably well for ^{97}Tc at all excitation energies. However, in contrast to KRK, the best fit GDR centroid energies vary between 15.0 MeV to 16.8 MeV.

All the experimental data for the decay of the CN ^{97}Tc are found to be in good agreement with the CASCADE prediction utilizing IST level density prescription. The extracted best fit E_{GDR} remains close to the value 15.6 MeV in agreement with the GDR systematics, except for $E_{\text{lab}} = 50$ MeV in which the estimated GDR peak energy is around 16.4 MeV. In all these data sets, the user dependent input \tilde{a} is taken as $A/8.0, A/9.7, A/9.0$ and $A/9.2$ MeV^{-1} at $E_{\text{lab}} = 28, 35, 42$ and 50 MeV, respectively, as extracted from the neutron evaporation data [19].

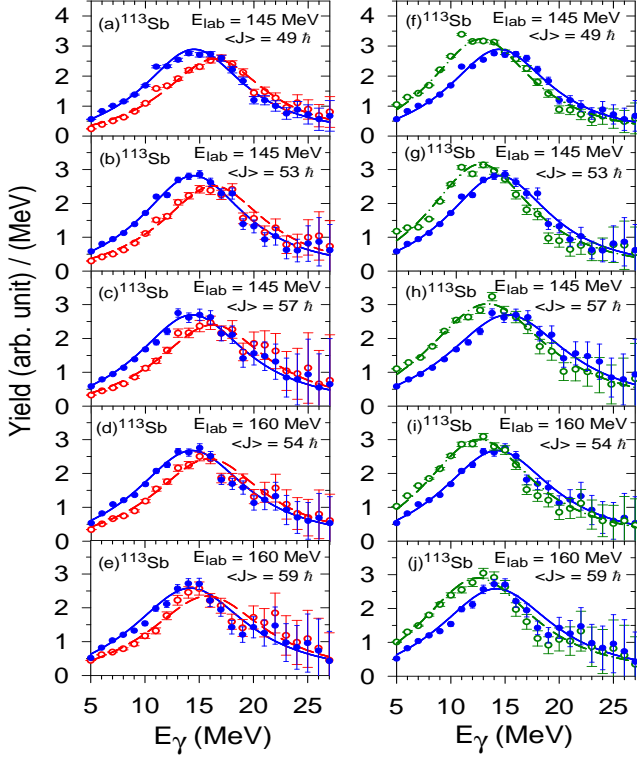


FIG. 6: (Color online) Panels (a) to (e): The experimental linearized plots for the reaction $^{20}\text{Ne} + ^{93}\text{Nb}$ at projectile energies 145 and 160 MeV along with CASCADE predictions utilizing KRK (open circles with red dashed line) and IST (filled circles with blue continuous line) level density formalisms. Panels (f) to (j): Same as above but utilizing BJK (open circles with green dotted-dashed line) and IST (filled circles with blue continuous line) level density formalisms.

C. ^{113}Sb

To understand the effect of level density prescriptions at higher angular momentum and higher excitation energy domains, the three level density prescriptions were used to explain the experimental data of high energy γ -rays measured for the compound nucleus ^{113}Sb [12]. The experimental data (open circles) along with KRK (red dashed line), BJK (green dotted-dashed line) and IST (blue continuous line) predictions are shown in the panels (a) and (b) of Fig 5 for $E_{\text{lab}}=145$ MeV ($E^*=109$ MeV) and average $J=53 \hbar$, $E_{\text{lab}}=160$ MeV ($E^*=121$ MeV) and average $J=54 \hbar$, respectively. The difference between KRK and IST predictions can be well understood through linearized plots shown in the left panels (a)-(e) of Fig 6 at $E_{\text{lab}}=145$ MeV and 160 MeV for different average CN angular momenta. Similarly, the right panels (f)-(j) of the same figure interpret the difference between IST and BJK predictions at similar projectile energies and average J . At higher J (49-59 \hbar) values, for IST prescription, the asymptotic level density parameter was not measured and therefore \tilde{a} is chosen as $A/8.0$

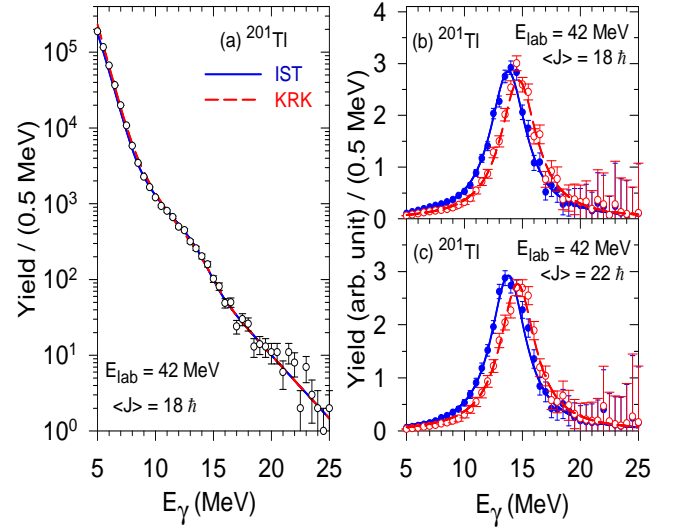


FIG. 7: (Color online) Panel (a) The experimental high energy γ -ray spectrum (open circles with error bars) for the reaction $^4\text{He} + ^{197}\text{Au}$ at projectile energy 42 MeV along with the CASCADE predictions exploiting KRK (red dashed line) and IST (blue continuous line) level density formalisms. Panels (b) and (c): The corresponding linearized plots.

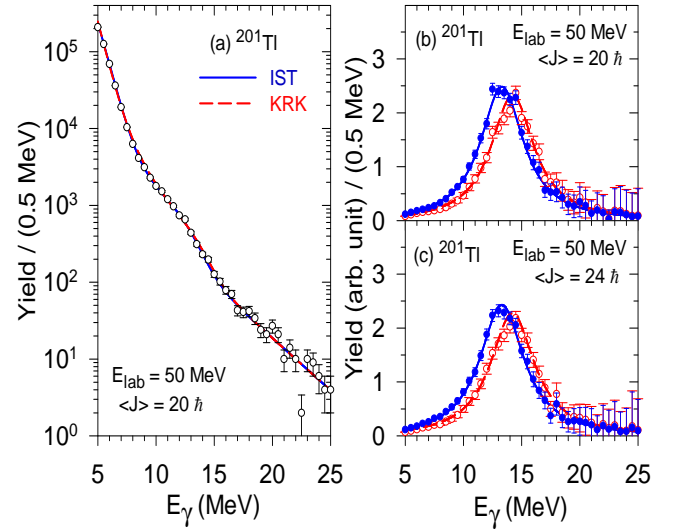


FIG. 8: (Color online) Panel (a) The experimental high energy γ -ray spectrum (open circles with error bars) for the reaction $^4\text{He} + ^{197}\text{Au}$ at projectile energy 50 MeV along with the CASCADE predictions exploiting KRK (red dashed line) and IST (blue continuous line) level density formalisms. Panels (b) and (c): The corresponding linearized plots.

MeV^{-1} according to Reisdorf formula [36]. The change in \tilde{a} from $A/8.0$ to $A/9.0 \text{ MeV}^{-1}$ could only alter the extracted E_{GDR} and S_{GDR} by 3% and 5%, respectively. For ^{113}Sb , IST prescription explains the experimental data very well and $E_{\text{GDR}} = 15.5 \text{ MeV}$ comes out to be consistent with the prediction (15.1 MeV) of the existing

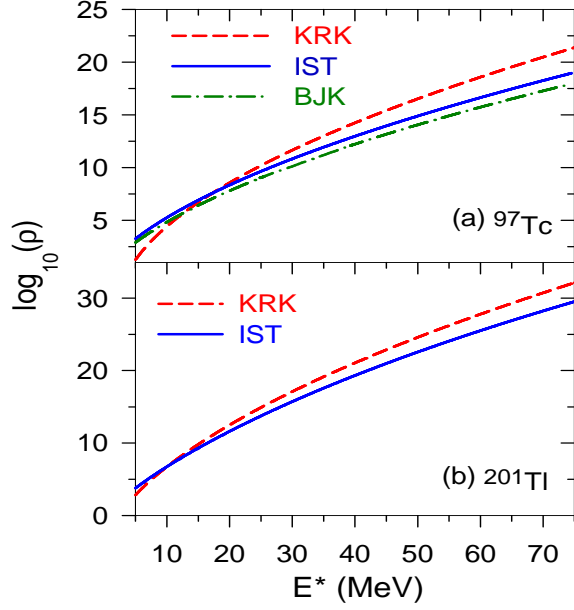


FIG. 9: (Color online) Panel (a): The angular momentum integrated level density as a function of excitation energy E^* for ^{97}Tc . The blue continuous, green dotted-dashed and red dashed lines show the level densities due to IST, BJK and KRK prescriptions. Panel (b): Same as above but for ^{201}Tl and considering IST and KRK prescriptions.

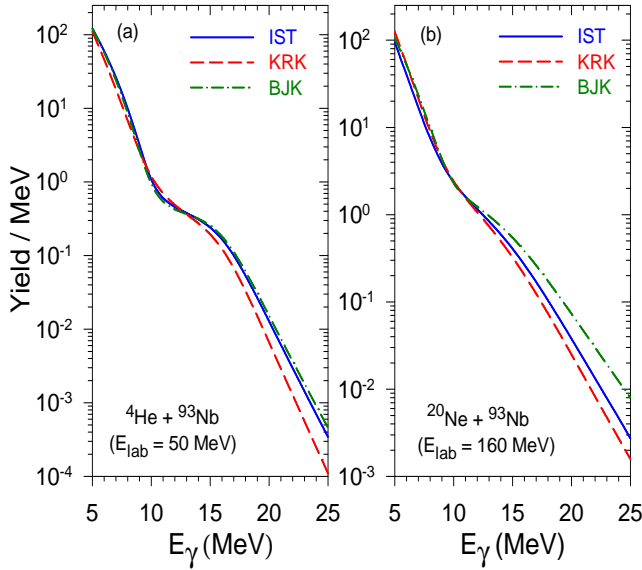


FIG. 10: (Color online) Panel (a): CASCADE outputs of high energy γ -ray spectrum for the reaction $^4\text{He} + ^{93}\text{Nb}$ at projectile energy $E_{lab} = 50$ MeV. The red dashed, blue continuous and green dotted-dashed lines correspond to the KRK, IST and BJK level density prescriptions, respectively. All the outputs are generated using same GDR parameters. Panel (b): Same as above but for $^{20}\text{Ne} + ^{93}\text{Nb}$ at projectile energy $E_{lab} = 160$ MeV.

systematics. However, KRK prescription can explain the data only if E_{GDR} is taken as 17.0-17.3 MeV, much larger than the existing systematics. BJK prescription can also explain the data but with much lower values of E_{GDR} (14.0 MeV).

D. ^{201}Tl

The suitability of three level density prescriptions were also investigated in higher nuclear mass region using another set of experimental data [17] for the reaction $^4\text{He} + ^{197}\text{Au}$ at $E_{lab} = 50$ MeV ($E^* = 47.5$ MeV) and $E_{lab} = 42$ MeV ($E^* = 39.5$ MeV) at lower compound nuclear J values (18-24 \hbar). The experimental high energy γ -spectra (open circles) are shown along with IST (blue continuous line) and KRK (red dashed line) prescriptions in the panels (a) of Fig. 7 and Fig. 8. The corresponding linearized plots are shown in (b) and (c) of Figs. 7 and 8. Again similar trend has been found in which KRK predicted best fit E_{GDR} comes out to be larger (14.4-14.7 MeV) than the excited state GDR centroid energy systematics (13.4 MeV), while IST predictions of E_{GDR} (13.5-13.9 MeV) remain in agreement with the systematics. In IST prescription, \tilde{a} was taken as $A/8.0$ MeV $^{-1}$. It was not possible to test BJK level density on the nucleus ^{201}Tl as it does not fall under the mass distribution of ^{252}Cf fission fragment.

E. Discussions

It is highly interesting to note that the high energy γ -ray spectra for all the four nuclei ^{63}Cu , ^{97}Tc , ^{113}Sb and ^{201}Tl at different excitation energies and angular momenta are described very well using the KRK and IST level density formalism in the CASCADE calculation. BJK prescription can explain only ^{97}Tc and ^{113}Sb data as the other two nuclei do not fall under the mass distribution of ^{252}Cf fission fragments. However, it is important to mention that the extracted GDR centroid energies come out to be very dissimilar using different level density prescriptions but the GDR widths remain unchanged in all the cases. The extracted values of GDR parameters for the three prescriptions are shown in table I.

Despite testing on varying experimental data with wide range of E^* & J and ground state shell correction energies, intriguingly, the KRK prescription consistently predicts higher values of E_{GDR} . The E_{GDR} for the nuclei ^{63}Cu , ^{97}Tc and ^{113}Sb with smaller ground state shell correction comes out to be 5, 13 and 12 % larger, respectively, than the existing systematics, while for ^{201}Tl with larger ground state shell correction energy this discrepancy is nearly 10 %. It is important to mention here that the KRK formalism is unique in comparison to the other two formalisms, as in this case the shell correction is incorporated through the nuclear excitation energy, in-

stead of modifying the level density parameter. Figs. 9a and 9b show calculated J -integrated KRK level density (red dashed line) as a function of excitation energy E^* along with the IST level density (blue continuous line) and BJK (green dot-dashed line) for the nucleus ^{97}Tc (small shell correction) and ^{201}Tl (large shell correction), respectively. As can be seen, KRK level density intersects IST at around $E^* = 20$ MeV and thereafter they diverge from each other. This seems to be the possible reason of agreement between KRK and IST predicted data only at the effective E^* (i.e E^* of 29.3 MeV minus the rotational energy) ~ 20 MeV for ^{97}Tc . In case of higher E^* , the two prescriptions differ. As it appears, the larger GDR centroid energy obtained, in comparison to the systematic, for KRK prescription could be due to incorrect extrapolation at higher E^* and J . In Fig. 10 the CASCADE predictions of high energy γ -ray spectra have been shown utilizing KRK (red dashed line), IST (blue continuous line) and BJK (green dot-dashed line) level density prescriptions for the nuclei ^{97}Tc at lower E^* & J and for ^{113}Sb at higher E^* & J . The GDR parameters were kept same for all the three prescriptions. The plots clearly indicate that for the common input parameters the KRK predicted γ -ray yield at higher energy side is lower compared to other two formalisms. This reduced yield is actually compensated by shifting E_{GDR} at higher energies resulting higher values of E_{GDR} . It is important to extract the correct centroid energy else it can introduce systematic error in the estimation of nuclear temperature for the GDR vibration. Apart from that a higher value of E_{GDR} would jeopardize the direct comparison between theoretical GDR lineshape and experimental GDR lineshape. Moreover, proper value of E_{GDR} is also very useful in the exploration of nuclear symmetry energy [23]. Hence, as it appears, the KRK level density prescription may not be used to explain the high energy γ -ray spectra as it systematically produces higher GDR centroid energy.

It can be fairly inferred that the BJK prediction matches well with the experimental data for different E^* values with reasonable best fit values of the GDR parameters, in so far as the nucleus ^{97}Tc is concerned, which has a very small amount of ground state deformation as well as lower shell correction energy. However, at higher J and higher E^* , BJK prescription misinterprets GDR centroid energies for ^{113}Sb (Fig. 9). The inherent problem of BJK formalism lies in the fact that the compiled level density parameters are independent of E^* . Therefore, for same mass number, one has to adopt the same set of level density parameter for all values of E^* . This does not have much effect on ^{97}Tc but has an adverse impact on the fitting of experimental spectra of ^{113}Sb . BJK prediction breaks down not only at higher E^* , but also in the event of high angular momentum. The discrepancy at higher E^* and J is also highlighted in Fig. 10b. As can

be seen, the BJK predicted γ -ray yield at higher energy side is much higher compared to other two formalisms for the common input GDR parameters. This higher yield is compensated by shifting E_{GDR} at lower values. Another disadvantage concerned with BJK is that the extracted level density parameters from the neutron decay in ^{252}Cf fission studies can be used reliably only for a system with same mass and deformation which is available in the BJK compilations. Therefore we could not use the BJK prescription in case of ^{63}Cu and ^{201}Tl . Moreover, BJK level density cannot be safely extrapolated for other systems, especially in case of deformed nucleus as observed earlier [30].

Interestingly, the IST level density formalism quite successfully describes the experimental data for all the four nuclei with reasonably correct values of E_{GDR} at all conditions of E^* & J and ground state shell correction. Therefore, it can be commented that among the three level density prescriptions the IST is most suitable. The reason being its efficiency to interpret the varying experimental data sets in terms of best fit GDR parameters in agreement with existing systematics.

In recent times, several new semi-empirical as well as microscopic level density formalisms have also been developed. Nakada and Alhassid calculated level densities [37] under the framework of Monte Carlo Shell Model for different nuclei. von Egidy and Bucurescu [38] also estimated level densities using Fermi gas model as well as constant temperature model. It will be interesting in future, if the applicability of newer level density formalisms can also be tested on high energy γ -ray spectra.

V. CONCLUSION

This work investigates the applicability of three different level density prescriptions viz. KRK, BJK and IST using experimental high energy γ -ray spectra for four nuclei ^{63}Cu , ^{97}Tc , ^{113}Sb and ^{201}Tl at different excitation energies and angular momenta. The extracted E_{GDR} in case of KRK prescription was found to be higher than that of the existing GDR systematics for all the four nuclei owing to the prediction of larger values of the nuclear levels at higher excitation energies in comparison to those predicted by other two formalisms. On the other hand, the BJK prescription predicted lower E_{GDR} compared to systematics in case of ^{113}Sb at higher E^* and J . Moreover, the BJK could not be tested on ^{63}Cu and ^{201}Tl due to its applicability in limited mass region. Intriguingly, the IST level density formalism quite successfully described all the data set both at low and high E^* and J indicating towards the universality of IST level density prescription in explaining the high energy γ -ray spectra with reasonably correct GDR parameters.

TABLE I: The GDR parameters extracted using different level density (l.d.) prescriptions.

CN	proj.	E_{lab} (MeV)	E^* (MeV)	J_{CN} \hbar	E_{GDR} (MeV) for l.d. formalisms			S_{GDR} for l.d. formalisms			Γ_{GDR} (MeV) for l.d. formalisms		
					BJK	KRK	IST	BJK	KRK	IST	BJK	KRK	IST
^{63}Cu	^4He	35	36.0	12 \pm 6		17.9 \pm 0.1	16.9 \pm 0.1		1.35	1.35		8.2 \pm 0.2	8.2 \pm 0.2
		35	36.0	14 \pm 6		17.9 \pm 0.1	16.8 \pm 0.1		1.75	1.75		8.0 \pm 0.2	8.0 \pm 0.2
		35	36.0	17 \pm 6		17.9 \pm 0.1	16.7 \pm 0.1		1.75	1.75		7.3 \pm 0.2	7.3 \pm 0.2
^{97}Tc	^4He	28	29.3	12 \pm 6	15.0 \pm 0.1	15.8 \pm 0.1	15.2 \pm 0.1	1.0	1.0	1.20	5.5 \pm 0.5	5.5 \pm 0.5	5.5 \pm 0.5
		35	36.0	13 \pm 4	15.5 \pm 0.1	17.0 \pm 0.1	15.6 \pm 0.1	1.1	1.35	1.25	6.0 \pm 0.5	6.0 \pm 0.5	6.0 \pm 0.5
		42	43.0	14 \pm 5	15.2 \pm 0.1	16.5 \pm 0.1	15.5 \pm 0.1	1.1	1.30	1.20	6.5 \pm 0.5	6.5 \pm 0.5	6.5 \pm 0.5
		50	50.4	14 \pm 5	16.8 \pm 0.1	17.5 \pm 0.1	16.4 \pm 0.1	0.9	1.10	1.10	7.5 \pm 0.5	7.5 \pm 0.5	7.5 \pm 0.5
^{113}Sb	^{20}Ne	145	109.0	49 \pm 11	14.0 \pm 0.2	17.4 \pm 0.2	15.5 \pm 0.2	1.0	1.0	1.0	11.6 \pm 0.3	11.6 \pm 0.3	11.6 \pm 0.3
		145	109.0	53 \pm 11	14.0 \pm 0.2	17.3 \pm 0.2	15.5 \pm 0.2	1.0	1.0	1.0	11.8 \pm 0.3	11.8 \pm 0.3	11.8 \pm 0.3
		145	109.0	57 \pm 11	14.0 \pm 0.2	17.3 \pm 0.2	15.5 \pm 0.2	1.0	1.0	1.0	12.4 \pm 0.3	12.4 \pm 0.3	12.4 \pm 0.3
		160	121.0	54 \pm 11	14.0 \pm 0.2	17.0 \pm 0.2	15.5 \pm 0.2	1.0	1.0	1.0	12.5 \pm 0.3	12.5 \pm 0.3	12.5 \pm 0.3
		160	121.0	59 \pm 11	14.0 \pm 0.2	17.0 \pm 0.2	15.5 \pm 0.2	1.0	1.0	1.0	13.0 \pm 0.3	13.0 \pm 0.3	13.0 \pm 0.3
^{201}Tl	^4He	42	39.5	18 \pm 6		14.8 \pm 0.3	13.9 \pm 0.3		1.0	1.0		3.8 \pm 0.5	3.8 \pm 0.5
		42	39.5	22 \pm 6		14.7 \pm 0.3	13.9 \pm 0.3		1.0	1.0		3.7 \pm 0.5	3.7 \pm 0.5
		50	47.5	20 \pm 6		14.4 \pm 0.3	13.5 \pm 0.3		1.0	1.0		4.5 \pm 0.5	4.5 \pm 0.5
		50	47.5	24 \pm 6		14.4 \pm 0.3	13.5 \pm 0.3		1.0	1.0		4.6 \pm 0.5	4.6 \pm 0.5

-
- [1] J. J. Gaardhoje, Ann. Rev. Nucl. Part. Sci. **42**, 483 (1992) .
- [2] K.A. Snover, Ann. Rev. Nucl. Part. Sci. **36**, 545 (1986).
- [3] M. N. Harakeh and A. van der Woude, Giant Resonances, Fundamental High-frequency Modes of Nuclear Excitation, Clarendon Press, Oxford, 2001.
- [4] Y. Alhassid, J. Zingman, and S. Levit, Nucl. Phys. **A469**, 205 (1987).
- [5] M. Kicińska-Habior et al., Phys. Rev. **C36**, 612 (1987).
- [6] A Bracco et al., Phys. Rev. Lett. **62**, 2080 (1989).
- [7] P. F. Bortignon et al., Phys. Rev. Lett. **67**, 3360 (1991).
- [8] W.E. Ormand et al., Phys. Rev. Lett. **69**, 2905 (1992).
- [9] Dimitri Kusnezov et al., Phys. Rev. Lett. **81**, 542 (1998).
- [10] M. P. Kelly et al., Phys. Rev. Lett. **82**, 3404 (1999).
- [11] A. Maj et al., Nucl. Phys. **A731**, 319 (2004).
- [12] Srijit Bhattacharya et al., Phys. Rev. **C77**, 024318 (2008).
- [13] D. R. Chakrabarty et al., J. Phys. G: Nucl. Part. Phys. **37**, 055105 (2010).
- [14] Deepak Pandit et al., Phys. Rev. **C81**, 061302(R)(2010).
- [15] S. Mukhopadhyay et al., Phys. Lett. **B709**, 9 (2012).
- [16] Deepak Pandit et al., Phys. Lett. **B690**, 473 (2010).
- [17] Deepak Pandit et al., Phys. Lett. **B713**, 434 (2012).
- [18] Deepak Pandit et al., Phys. Rev. **C87**, 044325 (2013).
- [19] Balaram Dey et al., Phys. Lett. **B731**, 92 (2014).
- [20] P. Heckman et al., Phys. Lett. **B555**, 43 (2003).
- [21] Nguyen Dinh Dang, Phys. Rev. **C84**, 034309 (2011).
- [22] Deepak Pandit et al., Phys. Rev. **C88**, 054327 (2013).
- [23] L. Trippa, G. Colo and E. Vigezzi, Phys. Rev. **C77**, 061304(R) (2008).
- [24] H. A. Bethe, Phys. Rev. **50**, 332 (1936).
- [25] F. Pühlhofer, Nucl. Phys. **A280**, 267 (1977).
- [26] W. Dilg, W. Schantl, H. Vonach, and M. Uhl, Nucl. Phys. **A217**, 269 (1973).
- [27] A. V. Ignatyuk, G. N. Smirenkin, and A. S. Tishin, Yad. Fiz. **21**, 485 (1975) Sov. J. Nucl. Phys. **21**, 255 (1975).
- [28] S. K. Kataria, V. S. Ramamoorthy and S. S. Kapoor, Phys. Rev. **C18**, 549 (1978).
- [29] C. Budtz-Jorgensen and H. H. Knitter, Nucl. Phys. **A490**, 307 (1988).
- [30] I. Dioszegi, I. Mazumdar, N. P. Shaw and P. Paul, Phys. Rev. **C63**, 047601 (2001).
- [31] S. Mukhopadhyay et al., Nucl. Instr. and Meth. **A582**, 603 (2007).
- [32] Deepak Pandit et al., Nucl. Instr. and Meth. **A624**, 148 (2010).
- [33] K. Banerjee et al., Nucl. Instr. and Meth. **A608**, 440 (2009).
- [34] H. Nifenecker, J. A. Pinston, Annu. Rev. Nucl. Part. Sci. **40**, 113 (1990).
- [35] J. R. Huizenga, H. K. Vonach, A. A. Katsanos, A. J. Gorski, and C. J. Stephen, Phys. Rev. **182**, 1149 (1969).
- [36] W. Reisdorf, Z. Phys. **A300**, 227 (1981).
- [37] H. Nakada and Y. Alhassid, Phys. Rev. Lett. **79**, 2939 (1997).
- [38] T. von Egidy and D. Bucurescu, Phys. Rev. **C72**, 044311 (2005).